Solar Energy 155 (2017) 478–489

Contents lists available at ScienceDirect

Solar Energy

journal homepage: www.elsevier.com/locate/solener

An improved single-diode model parameters extraction at different operating conditions with a view to modeling a photovoltaic generator: A comparative study

Abdelkader Abbassi [a,*], Rabiaa Gammoudi [b], Mohamed Ali Dami [a], Othman Hasnaoui [b], Mohamed Jemli [a]

[a] University of Tunis, Higher National Engineering School Of Tunis (ENSIT), Engineering Laboratory of Industrial Systems and Renewable Energies (LISIER), 5 avenue Taha Hussein, PO Box 56, 1008 Tunis, Tunisia

[b] University of Carthage, National Institute of Applied Sciences of Tunisia (INSAT), Unit of Research (ERCO), North Urban Center, 1080 Tunis Cedex, Tunisia

ARTICLE INFO

Article history:
Received 21 January 2017
Received in revised form 12 April 2017
Accepted 24 June 2017
Available online 29 June 2017

Keywords:
Parameters extraction
Photovoltaic (PV) panel
Performance evaluation
Newton-Raphson algorithm
Genetic Algorithm (GA) approach
Accuracy

ABSTRACT

This paper proposes advanced analytical, numerical and genetic algorithm (GA) approaches for retrieving the parameters of photovoltaic (PV) panel. A comparative study for extracting the five parameters of a single diode PV model is presented. Based on the datasheet values, a numerical based Newton-Raphson algorithm is investigated for solving the current-voltage relation of a single diode solar PV model. To highlight the rigorous performance of our models, a second analytical model is proposed. For improving the accuracy of solar panel parameters, a technique based on GA is established. This approach is based on the problem of research and optimization of the extracted parameters as an objective function. To account for variation in solar radiation and temperature, these models are presented under the reference and real operating conditions. The performances of the proposed algorithms are compared by using MATLAB scripts programming, and the theoretical advantages of GA model were demonstrated. The different models are validated experimentally by various tests of temperature and solar irradiance variation. The experimental results indicate that the GA model has a very satisfactory performance compared with the two other models and it offers good compromise between accuracy and fastness.

1. Introduction

During last twenty years, solar energy, like wind energy, is one of the most attractive concerns. Due to the intensive presence of the Saharan climate especially in Africa, solar energy must be among the best renewable sources that have gained great popularity due to its high availability and predictability. With the trend to serve exponential demand for electricity as their economies grow, the production of electricity from solar energy sources has a great interest to developing countries, especially because it has many isolated and remote regions from electricity distribution networks. To solve this problem, a highest priority must be accorded to the exploitation of the solar potential must be a priority.

From its discovery, the conversion of solar energy into electrical energy using photovoltaic modules reveals an undesirable problem. The non-linearity of the photovoltaic modules outputs, presents today a very respectful occupation of the researchers.

In order to describe the behavior of photovoltaic cells, Different models based on the current-voltage curve of a P-N junction were used. Recently, various researches on the prediction of the current-voltage characteristic curve are founded in the literature (Salaux et al., 2011). In this context, the two diodes model is known as the most accurate model for representing the equivalent electrical circuit of a photovoltaic cell.

Nevertheless, additional difficulties and a longer calculation time are appended to solving the basic equation describing the two diodes model, since their parameters are defined in a nonlinear manner (Ishaque et al., 2011a, 2011b). As the most commonly used, the single diode model can be categorized into two main types (Dongue et al., 2012). The simplified four-parameter model neglecting shunt resistance by assuming it as infinite value in the equivalent electrical circuit and the five-parameter model that characterizes the current-voltage curve of the cell by maintaining the effect of the shunt resistor. The five-parameter model evaluates the photocurrent, the saturation current, the series and shunt resistors and the ideality factor of the diode.

Various methods are conceivable to determine the parameters of the equivalent electric circuit of a solar cell. However, the

* Corresponding author.
E-mail addresses: abd_abbassi@yahoo.com (A. Abbassi), medali.dami@esstt.rnu.tn (M. Ali Dami), mohamed.jemli@ensit.rnu.tn (M. Jemli).

http://dx.doi.org/10.1016/j.solener.2017.06.057
0038-092X/

equation that links the different parameters which make up the current-voltage relationship is defined in a non-linear manner or implied by mathematical relationships. To solve this problem, several techniques can be considered:

Taking into account the nonlinearity relationship which cannot easily expressed of the solar panel parameters. A first approach consists to resolve this relation by the artificial neural network method (Singh et al., 2014); this approach is used to predict the parameters of the electrical equivalent circuit of a photovoltaic cell. Another approach consists on calculating the parameters of the PV cell by the Newton-Raphson method (Bogning Dongue et al., 2013; Ma et al., 2014; Chouder et al., 2012; Bellia et al., 2014; Bonkoungou et al., 2015); that operators in an iterative manner and requires the initialization of parallel and series resistors while other parameters are defined referring to the photovoltaic modules manufacturer data.

In (Ishaque et al., 2011b; Ishaque and Salam, 2011; Siddiqui and Abido, 2013; Peng et al., 2013), the authors have investigated an improved modeling version based on different types of Evolutionary Algorithms (EA) to determine the photovoltaic module parameters. Besides, three algorithms are employed such as the particle swarm optimization (PSO), the Genetic Algorithm (GA) Ismail et al., 2013 and the Differential Evolution (DE). The purpose of these algorithms was to determine the parameters of the electrical equivalent model of photovoltaic cells. A critical study makes it possible to judge the stochastic optimization method as the most efficient one. In addition, a Bird Mating Optimizer (BMO) approach was used in Askarzadeh (2015) to estimate the model electrical parameters of an amorphous silicon PV module under different operating conditions.

Some analytical propositions are also suggested in this subject. In fact, an efficient analytical approach for obtaining a five parameters model of photovoltaic modules using only reference data is proposed by Lo Brano (2013), Chikh and Chandra (2015). Herein, the electrical behaviors of the photovoltaic model depending on the operation conditions of temperature and solar irradiance were described analytically. In (Batzelis and Papathanassiou, 2016; Hejri et al., 2014), various analytical solutions for approximating the parameters of the single diode and the double diode models of a photovoltaic module have been presented, respectively. Based on manufacturer's datasheet, various numerical algorithms are investigated for solving the current-voltage equation of a single diode solar PV model (Ayodele et al., 2016; Silva et al., 2016). Other numerical methods, which are based on Newton-Raphson and Levenberg-Marquard algorithms, are proposed in Appelbaum and Peled (2014).

In addition, based on the parameters extraction of solar cells, review papers have also addressed this issue (Humada et al., 2016; Jordehi, 2016; Lineykin et al., 2014; Ciulla et al., 2014). These works have focused on the extraction of the DC parameters of solar cells by a set of techniques based on both single-diode and double-diode models is described and discussed. Moreover, the existing research works on solar cell model parameter estimation problem are classified in a fair manner into different categories.

In this paper, a single diode model which depends on the solar irradiance, the temperature and five characteristics parameters is established. Analytical and numerical studies were developed to solve the nonlinearity behavioral in order to determine the five parameters of PV panel. A technique based on GA model is proposed for improving the accuracy of the extracted parameters describing the electrical equivalent model of the solar panel. Some experimental tests have been conducted in order to better choose the most suitable model. After comparison of the different proposed models with the experimental data, the results show that the GA model is almost confused with these data. This model offers a good compromise between fastness and accuracy.

The rest of this paper is structured as follows. Section 2 is related to a preface on the modeling of the PV system. Section 3 describes the parameters extraction under reference conditions, which includes the different models used in this study. In Section 4, the parameters determination under real conditions is demonstrated. Section 5 discusses the obtained results and their comparison with experimental ones. Finally, Section 6 outlines the main conclusions.

2. Mathematical modeling of a photovoltaic module

Although a multitude of models and techniques have been published in the literature, the modeling of a photovoltaic generator remains a complex undertaking. In order to resolve this problem electrically, various models are used to describe the I-V curve variation, on which we look at three characteristic points to improve the relationship between all components of electrical equivalent circuit.

In this work, based on the variation of solar radiation and temperature, different models are discussed to get the current-voltage and the power-voltage characteristics. Analytical, numerical and GA based evolutionary computational approaches have been used. The synoptic scheme of PV parameters extraction is depicted in Fig. 1.

This one shown below was judged as the most appropriate, following an exhaustive research on this subject (Abbassi and Chebbi, 2012; Ma et al., 2014; Abbassi et al., 2017; Mares et al., 2015). The objective of this segment is not only to describe in detail the equations of this model, but also to highlight the shortcomings with respect to this research theme and to propose modifications to enable them to be filled.

Fig. 2 shows the equivalent electrical circuit of a single diode model of photovoltaic generator. It consists of a current source I_{ph}, a diode D, a series resistor R_s and a shunt resistor R_{sh}.

The current-voltage relation of photovoltaic cell is given by:

$$I = I_{ph} - I_D - I_{sh} = I_{ph} - I_0\left(e^{\left(\frac{V+R_sI}{V_t}\right)} - 1\right) - \frac{V + R_sI}{R_{sh}} \quad (1)$$

The diode thermal voltage at reference conditions is given by:

$$V_t = \frac{AkT}{q} \quad (2)$$

where I_{ph} is the photo current (A); I_0 is the diode saturation current (A); A is the diode ideality factor; k is the Boltzmann constant ($1.38 \cdot 10^{-23}$ J/K); q is the electron charge ($1.6 \cdot 10^{-19}$ C); T is the cell temperature (K); R_s is the series resistance (Ω) and R_{sh} the shunt resistance (Ω).

In Eq. (1), the five parameters which defined the current-voltage relation of photovoltaic cell, vary in accordance with the solar irradiance, the cell temperature and necessary with their reference values.

The particulars points of current voltage, power-voltage characteristics of the solar panel used in this work are represented in Fig. 3.

3. Calculating parameters procedure under reference conditions

3.1. Analytical approach

The current voltage relation which described by Eq. (1), in the reference conditions, as follows:

$$I = I_{phref} - I_{0ref}\left(e^{\left(\frac{V+R_{sref}I}{V_{tref}}\right)} - 1\right) - \frac{V + R_{sref}I}{R_{shref}} \quad (3)$$

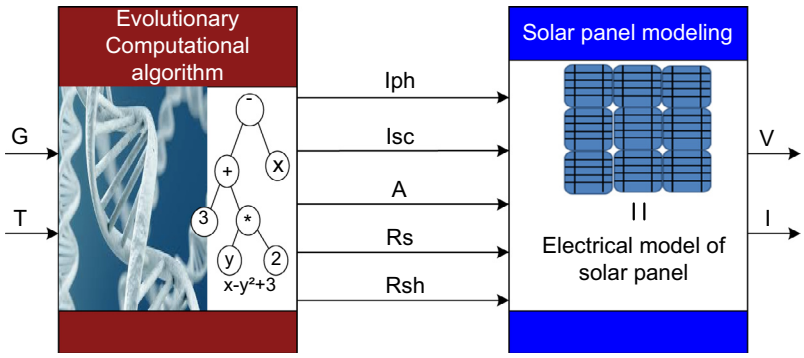

Fig. 1. Synoptic scheme of PV parameters extraction.

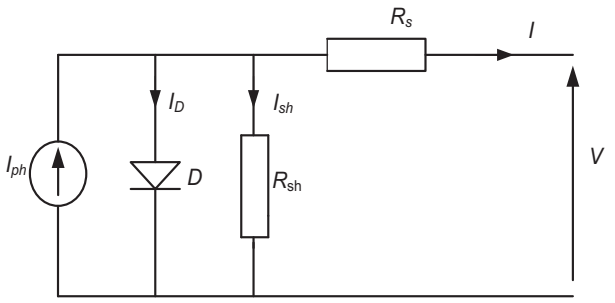

Fig. 2. Equivalent electrical circuit of a single-diode model.

where I_{phref}, I_{0ref}, V_{tref}, R_{sref} and R_{shref} are evaluated in a particular point of current-voltage characteristics curve represented in Fig. 3, such as:

In the short circuit point: $I = I_{sc}$, $V = 0$

$$I_{scref} = I_{scmes} * (G_{ref}/G_{mes}) + \alpha I_{sc} * (T_c - T_{ref}) \quad (4)$$

In the open circuit point: $I = 0$, $V = V_{0c}$

$$V_{0cref} = V_{0cmes} - \beta * (T_c - T_{ref}) + V_t * \ln * (G_{ref}/G_{mes}) \quad (5)$$

In the maximum power point: $V = V_m$, $I = I_m$

$$I_{mref} = I_{mmes} * (G_{ref}/G_{mes}) + \alpha * (T_c - T_{ref}) \quad (6)$$

$$V_{mref} = V_{mmes} - \beta * (T_c - T_{ref}) - R_{smes} * (I_{mmes} - I_{mref}) + V_t * \ln * (G_{ref}/G_{mes}) \quad (7)$$

where I_{scmes}, V_{0mes} are the measured short circuit current and open circuit voltage respectively, I_{mmes} and V_{mmes} are the current and voltage at maximum power point tracking, G_{ref} and G_{mes} are the reference and the measured solar irradiance respectively, α is the temperature coefficient of short circuit current, β is the temperature coefficient of open circuit voltage, T_c and T_{ref} are the measured and reference temperature respectively, R_{smes} is the measured series resistance and V_t is the diode thermal voltage.

Now, and after describing the key parameters of the photovoltaic cell, we can define firstly the unknown five reference parameters as follows:

The diode ideality factor:

$$A_{ref} = \frac{V_{tref} q}{k T_{ref}} \quad (8)$$

where

$$V_{tref} = \frac{V_{mref} + I_{mref} R_{sref} - V_{0cref}}{\left[\ln\left(I_{scref} - \left(\frac{V_{mref}}{R_{shref}}\right) - I_{mref}\right) - \ln\left(I_{sref} - \left(\frac{V_{0cref}}{R_{shref}}\right)\right) - \left(\frac{I_{mref}}{I_{scref} - \frac{V_{0cref}}{R_{shref}}}\right)\right]} \quad (9)$$

The dark saturation current:

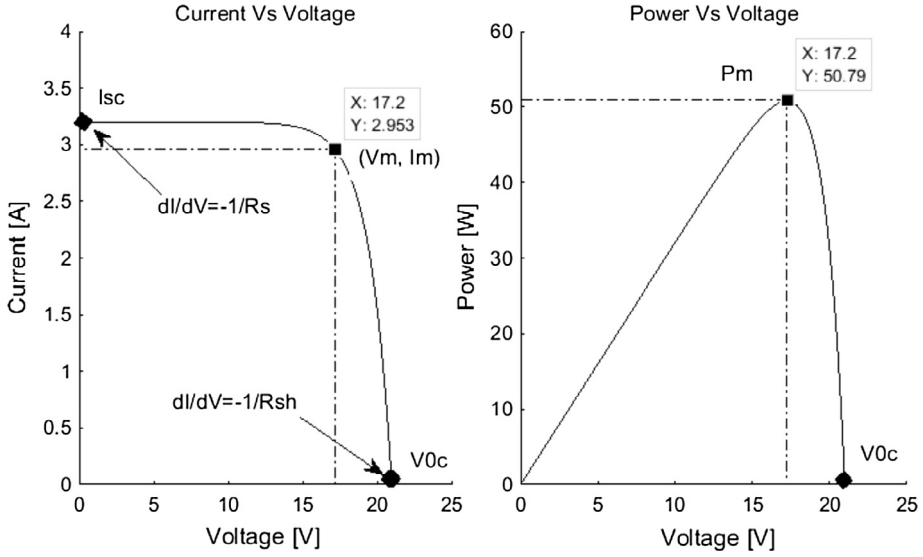

Fig. 3. Current-Voltage, Power-Voltage Characteristics and relationship between current-voltage, R_s and R_{sh}.

$$I_{0ref} = (I_{scref} - V_{0cref}/R_{shref})e^{\left(-\frac{V_{0ref}}{V_{tref}}\right)} \quad (10)$$

The series and shunt resistances:

$$R_{shref} = R_{sh0} \quad (11)$$

$$R_{sref} = R_{s0} \quad (12)$$

The diode ideality factor:

$$I_{phref} = I_{scref}\left(1 + \frac{R_{sref}}{R_{shref}}\right) + I_{0ref}\left(e^{\left(\frac{I_{scref}R_{sref}}{V_{tref}}\right)} - 1\right) \quad (13)$$

where R_{s0} and R_{sh0} are given by the manufacture of photovoltaic module at standard test conditions STC (1000 W/m^2 of solar irradiance and 25 °C of cell temperature).

All different parameters of TITAN-12-50 solar panel in three characteristics points: open circuit (V_{0c}, 0); short circuit (0, I_{sc}); maximal power (V_m, I_m) and their temperature coefficients are illustrated in Table 1.

3.2. Numerical approach

The general I-V characteristics of PV panel based on the single diode model is expressed by Eq. (1). In the reference conditions, we can put the current voltage relation described by Eq. (1) in the following form (Ishaque et al., 2011a, 2011c):

$$I = I_{phref} - I_{0ref}\left(e^{\left(\frac{V+R_{sref}I}{V_{tref}}\right)} - 1\right) - \frac{V + R_{sref}I}{R_{shref}} \quad (14)$$

where I_{phref}, I_{0ref}, V_{tref}, R_{sref} and R_{shref} are evaluated in a particular point of current-voltage characteristics curve represented in Fig. 3, such as:In the short circuit point: I = I_{sc}, V = 0

$$I_{scref} = I_{phref} - I_{0ref}\left(e^{\left(\frac{R_{sref}I_{scref}}{V_{tref}}\right)} - 1\right) - R_{sref}\frac{I_{scref}}{R_{shref}} \quad (15)$$

In the open circuit point: I = 0, V = V_{0c}

$$I_{phref} - I_{0ref}\left(e^{\left(\frac{V_{0cref}}{V_{tref}}\right)} - 1\right) - \frac{V_{0cref}}{R_{shref}} = 0 \quad (16)$$

In the maximum power point: V = V_m, I = I_m

$$I_{mref} = I_{phref} - I_{0ref}\left(e^{\left(\frac{V_{mref}+R_{sref}I_{mref}}{V_{tref}}\right)} - 1\right) - \frac{V_{mref} + R_{sref}I_{mref}}{Rshref} \quad (17)$$

In Eq. (14), the derivative of the current with respect to the voltage at the open circuit voltage is equivalent to the series resistance R_{sref} under standard test conditions:

$$\left.\frac{dI}{dV}\right|_{\substack{I=0\\V=V_{0cref}}} = -\frac{1}{R_{sref}} \quad (18)$$

Table 1
The key specifications of the TITAN-12-50 PV module.

Characteristics	Value
Short circuit current I_{sc} (A)	3.2
Open circuit voltage V_{0c} (V)	21
Maximum Power P_m (W)	50
Current at maximum power point I_m (A)	2.9
Voltage at maximum power point V_m (V)	17.2
Temperature coefficient of short circuit current (α)	+0.1%/°C
Temperature coefficient of open circuit voltage (β)	−0.38%/°C
Temperature coefficient of maximum power (γ)	−0.47%/°C
NOCT	45 ± 0.2
Cells number connected in series	36

In Eq. (14), the derivative of the current with respect to the voltage at the short circuit current is equivalent to the series resistance R_{shref} under standard test conditions:

$$\left.\frac{dI}{dV}\right|_{\substack{I=I_{scref}\\V=0}} = -\frac{1}{R_{shref}} \quad (19)$$

where I_{scref} is the short circuit current at STC, V_{0ref} is the open circuit voltage at STC, V_{mref} is the voltage at the maximum power point MPP at STC, I_{mref} is the voltage at the maximum power point MPP at STC.

The above parameters are normally provided by the datasheet manufacturer's. At MPP, the derivative of the power with respect to the voltage is equal to zero, and it's given by:

$$\left.\frac{dP}{dV}\right|_{\substack{I=I_{mref}\\V=V_{mref}}} = 0 \quad (20)$$

From Eq. (16), the photo current generated I_{phref} can be obtained as:

$$I_{phref} = I_{0ref}\left(e^{\left(\frac{V_{0cref}}{V_{tref}}\right)} - 1\right) - \frac{V_{0cref}}{R_{shref}} \quad (21)$$

Substituting Eq. (21) into Eq. (15) yields:

$$I_{scref} = I_{0ref}\left(e^{\left(\frac{V_{0cref}}{V_{tref}}\right)} - e^{\left(\frac{R_{sref}I_{scref}}{V_{tref}}\right)}\right) + \frac{V_{0cref} - I_{scref}R_{sref}}{R_{shref}} \quad (22)$$

After simplification in Eq. (22), we will find:

$$I_{scref} = I_{0ref}\left(e^{\left(\frac{V_{0cref}}{V_{tref}}\right)}\right) + \frac{V_{0cref} - I_{scref}R_{sref}}{R_{shref}} \quad (23)$$

Solving this equation for I_{0ref}, results in:

$$I_{0ref} = (I_{scref} - \frac{V_{0cref} - I_{scref}R_{sref}}{R_{shref}})e^{\left(-\frac{V_{0cref}}{V_{tref}}\right)} \quad (24)$$

Substituting Eqs. (24) and (21) into Eq. (17) allows:

$$I_{mref} = I_{0ref} - \frac{V_{mref} + R_{sref}I_{mref} - R_{sref}I_{scref}}{R_{shref}} - (I_{0ref} - \frac{V_{0cref} - R_{sref}I_{scref}}{R_{shref}})\left(e^{\left(\frac{V_{mref}+R_{sref}I_{mref}}{V_{tref}}\right)}\right) \quad (25)$$

Eq. (20) can be rewritten as:

$$\left.\frac{dP}{dV}\right|_{\substack{I=I_{mref}\\V=V_{mref}}} = \frac{d(IV)}{dV} = I + \frac{dI}{dV}V = 0 \quad (26)$$

Eq. (14) is a transcendent equation, which needs numerical method to express the current and voltage. Therefore, it's rewritten as:

$$I = f(I, V) \quad (27)$$

By differencing Eq. (27), we obtain the following equation:

$$dI = df(I, V) = dI\frac{\partial f(I,V)}{\partial I} + dV\frac{\partial f(I,V)}{\partial V} \quad (28)$$

Therefore:

$$\frac{dI}{dV} = \frac{\frac{\partial f(I,V)}{\partial V}}{1 - \frac{\partial f(I,V)}{\partial I}} \quad (29)$$

From (29) and (26), we obtain:

$$\left.\frac{dP}{dV}\right|_{\substack{I=I_{mref}\\V=V_{mref}}} = \frac{d(IV)}{dV} = I_{mref} + \frac{\frac{\partial f(I,V)}{\partial V}}{1 - \frac{\partial f(I,V)}{\partial I}}V_{mref} \quad (30)$$

From the above:

$$\left.\frac{dP}{dV}\right|_{\substack{I=I_{mref}\\V=V_{mref}}} = I_{mref} + V_{mref} \times \left(\frac{ -\left(I_{0ref} - \frac{V_{0cref} - R_{sref} I_{scref}}{R_{shref}}\right) e^{\left(\frac{V_{mref} + R_{sref} I_{mref}}{V_{tref}}\right)} }{ V_{tref} R_{shref} } - \frac{1}{R_{shref}} \right) \Bigg/ \left(1 + \frac{ (I_{0ref} - \frac{V_{0cref} - R_{sref} I_{scref}}{R_{shref}}) e^{\left(\frac{V_{mref} + R_{sref} I_{mref}}{V_{tref}}\right)} }{ V_{tref} R_{shref} } - \frac{R_{sref}}{R_{shref}} \right) \tag{31}$$

There are two Eqs. (31) and (25) with three unknowns, which are R_s, R_{sh} and A_{ref}. Eq. (19) can be used as the third equation. Eqs. (19), (30) and (31) lead to:

$$-\frac{1}{R_{shref}} = \frac{ -\left(I_{0ref} - \frac{V_{0cref} - R_{sref} I_{scref}}{R_{shref}}\right) e^{\left(\frac{V_{mref} + R_{sref} I_{mref}}{V_{tref}}\right)} }{ V_{tref} R_{shref} } - \frac{1}{R_{shref}} \Bigg/ \left(1 + \frac{ (I_{0ref} - \frac{V_{0cref} - R_{sref} I_{scref}}{R_{shref}}) e^{\left(\frac{V_{mref} + R_{sref} I_{mref}}{V_{tref}}\right)} }{ V_{tref} R_{shref} } - \frac{R_{sref}}{R_{shref}} \right) \tag{32}$$

It's possible now to determine the five unknown parameters, which are I_{phref}, I_{0ref}, R_{sref}, R_{shref} and A_{ref} by using Eqs. (21), (23), (25), (31) and (32).

The Newton Raphson method has been widely used for obtaining the roots of implicit transcendental equations and is popular in iterative computer applications because of its simplicity and rapid convergence. In this study, these five equations obtained were solved using the Newton Raphson method on the basis of the initial proposed values. When the numerical solution is done with the Newton Raphson method, a tolerance value *Tol* has been identified as the rule for stopping the iterations, and the iterations continued until the difference between the calculated power and that obtained experimentally fell under this value.

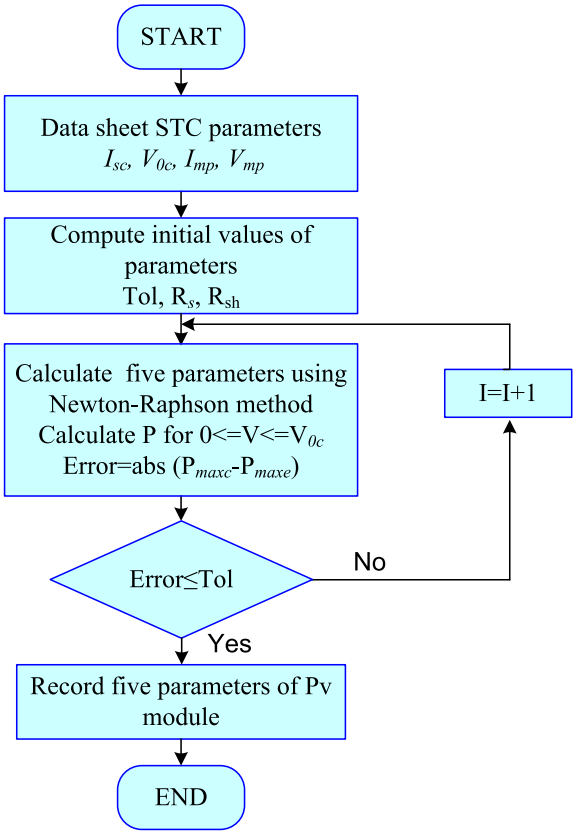

Fig. 4. Flow-chart of Newton-Raphson algorithm.

It is pivotal to start with an appropriate initial value for numerical solutions. Otherwise, the number of iterations increases and, in some cases, the numerical solution cannot converge to the result. As mentioned in the flowchart, only the values of the data sheet were used as a first step when these calculations have been done. Thus, the initial values should be very close to the real values. For this we started by setting a very small value of the tolerance and initialized the values of the shunt and series resistances.

In this section, the values of the Iphref, I0ref, Rsref, Rshref and Aref parameters were calculated using Eqs. (21), (23), (25), (31) and (32) previously developed. The calculation of the values of the parameters and of the drawing of the I-V, P-V characteristics was carried out. The flowchart of the developed program is given in Fig. 4.

In this work, a based Newton-Raphson algorithm is developed. The five parameters of the PV module depicted above can be arranged in the following matrix form, respectively:

$$x = \begin{bmatrix} x_1 \\ x_2 \\ x_3 \\ x_4 \\ x_5 \end{bmatrix}, \quad F(x) = \begin{bmatrix} f_1 \\ f_2 \\ f_3 \\ f_4 \\ f_5 \end{bmatrix} \tag{33}$$

Newton-Raphson method is a numerical technique which is established to estimate the five parameters of a single diode model in the form of F(x) = 0, where x is the array of the five parameters as in Eq. (33). F(x) and the Jacobian matrices J(x) are derived from previous five-equation as follow:

$$J(x) = \begin{bmatrix} \frac{\partial f_1}{\partial x_1} & \frac{\partial f_1}{\partial x_2} & \frac{\partial f_1}{\partial x_3} & \frac{\partial f_1}{\partial x_4} & \frac{\partial f_1}{\partial x_5} \\ \frac{\partial f_2}{\partial x_1} & \frac{\partial f_2}{\partial x_2} & \frac{\partial f_2}{\partial x_3} & \frac{\partial f_2}{\partial x_4} & \frac{\partial f_2}{\partial x_5} \\ \frac{\partial f_3}{\partial x_1} & \frac{\partial f_3}{\partial x_2} & \frac{\partial f_3}{\partial x_3} & \frac{\partial f_3}{\partial x_4} & \frac{\partial f_3}{\partial x_5} \\ \frac{\partial f_4}{\partial x_1} & \frac{\partial f_4}{\partial x_2} & \frac{\partial f_4}{\partial x_3} & \frac{\partial f_4}{\partial x_4} & \frac{\partial f_4}{\partial x_5} \\ \frac{\partial f_5}{\partial x_1} & \frac{\partial f_5}{\partial x_2} & \frac{\partial f_5}{\partial x_3} & \frac{\partial f_5}{\partial x_4} & \frac{\partial f_5}{\partial x_5} \end{bmatrix} \tag{34}$$

$$y_n = -J^{-1} F(x_n) \tag{35}$$

$$x_{n+1} = x_n + y_n \tag{36}$$

3.3. Genetic algorithm approach

The genetic algorithm (GA) is based on the theory of evolutionary biology (Ishaque et al., 2011b). The ordinary operators used to evaluate step by step this conventional algorithm are set out as follows (Ishaque et al., 2011b; Ismail et al., 2013):

3.3.1. Selection

This procedure selects the chromosomes that contribute to the reproductive process to give birth to the next generation, only the best chromosomes are considered for the next generation.

3.3.2. Mutation

This procedure is performed by the GAs to explore new solutions and it introduces a modification in certain genes of a chromosome in a population. A mutation can randomly affect any gene, any cell, at any time. Random mutations alter a small percentage of the population with the exception of the best chromosomes. If the mutation rate is greater than 20%, too many good parameters can be mutated, causing the algorithm to stop. Note that the new value of each parameter should be in the corresponding range [XiL, XiH]. Therefore, mutated parameters are engaged to ensure that the parameters space is explored in new regions.

3.3.3. Crossover

This process uses two selected chromosomes of a current generation (the parents) and crosses them with a certain probability of crossing to obtain two different individuals giving rise to a progeny that carries part of the genetic material of each parent for the new generation. Parent organisms must be genetically compatible and may be of different varieties or closely related species. There are several types of crossover, but the simplest method is to arbitrarily choose one or more points in the chromosome of each parent to mark as crossing points. Consequently, the parameters between these points are simply exchanged between the two parents.

3.3.4. Objective function

The output current of the PV panel is well known and can be described as:

$$I_t = I_{ph} - I_0\left[\exp\left(q\frac{V_t + R_s I_t}{AkT}\right) - 1\right] - \frac{V_t + R_s I_t}{R_{sh}} \quad (37)$$

To apply the GA methods, Eq. (37) has to be re-written as:

$$f(V_t, I_t, z) = I_t - I_{ph} + I_0\left[\exp\left(q\frac{V_t + R_s I_t}{AkT}\right) - 1\right] + \frac{V_t + R_s I_t}{R_{sh}} \quad (38)$$

where z = [R_s R_{sh} I_{ph} I_0 A] are the parameters set to extract. After each iteration, the values in z is updated and then checked if it has converge to the correct value. The procedure ends when intended maximum number of iteration has been reached.

To objectively evaluate the performance of the GA method, an objective function j is introduced. The objective function used in this work can be given by:

$$j = \text{Min RMSE} = \sqrt{\frac{1}{N}\sum_{1}^{N}(F(V_t, I_t, z))^2} \quad (39)$$

Subject to

$$R_{smin} \leqslant R_s \leqslant R_{smax}$$

$$R_{shmin} \leqslant R_{sh} \leqslant R_{shmax}$$

$$I_{phmin} \leqslant I_{ph} \leqslant I_{phmax}$$

$$I_{0min} \leqslant I_0 \leqslant I_{0max}$$

$$A_{min} \leqslant A \leqslant A_{max}$$

where V_t and I_t are the data of I–V characteristics curve, respectively; N is the number of data. Hence, the optimization algorithm is based on the minimization of the fitness function with respect to the parameters interval. A smaller value of j implies the least deviation between the I, V data and the one computed by the GA method.

In this algorithm, the initial generation of the population is formed by randomly generating the population members. Each possible solution is a code of the decision vector, taking into account the upper and lower constraints. This initial generation evolves through successive iterations, and the members of each generation are evaluated in order to calculate the objective function j, the member having the least error being selected.

For the model of a single diode, the decision vector is z = [R_s R_{sh} I_{ph} I_0 A]. The lower and upper constraints for some of the construction vector variables of the decision vector are common to the different types of photovoltaic modules, while the remaining variables have lower and higher constraints, depending on the PV type and the manufacturer.

In this study, the ideality factor of the diodes A has lower and upper constraints between 1 and 2. The R_s series resistance generally has lower and upper constraints between 0.05 Ω and 1 Ω,

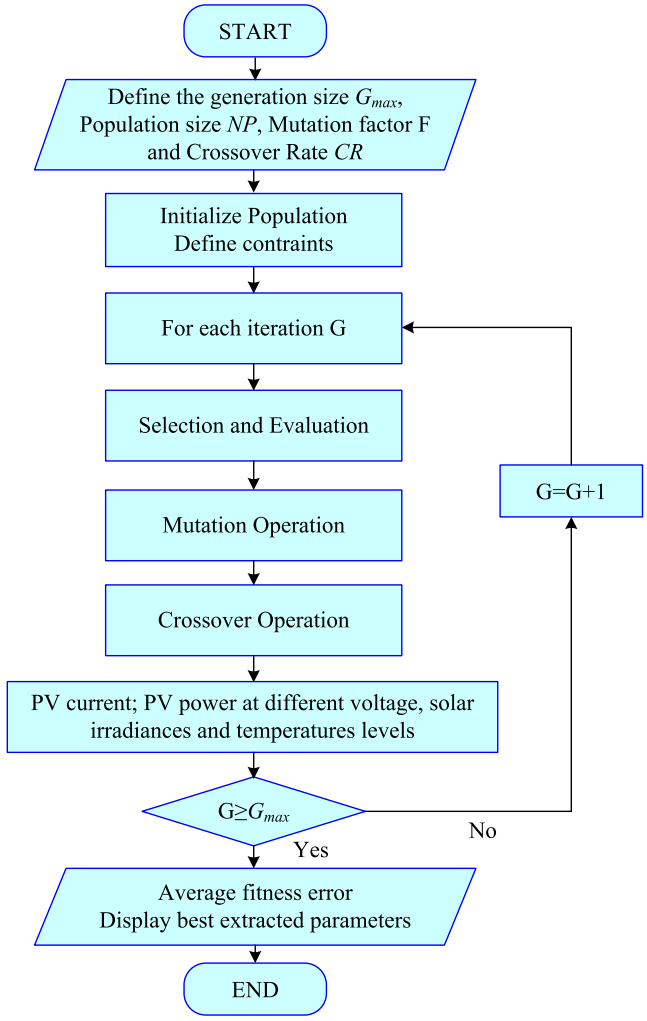

Fig. 5. Flow-chart of Genetic Algorithm.

Whereas the shunt resistance R_{sh} is usually has lower and upper constraints between 50 Ω and 200 Ω, but these values can be modified as a function of the results of the genetic algorithm. The optimal solution is obtained when a precise number of generations reach the maximum generation size Gmax and the best extracted parameters are displayed.

In this method, and after many executions, it has been found that a population size of 60 is adequate for the purposes of this article, while the number of generations needed to give the most optimal solution is more than 100. Fig. 5 details the flowchart of the genetic algorithm process.

4. Parameters processing in general conditions

For fixed values of irradiation and temperature, the I-V characteristics of the photovoltaic system describe its static behavior. A dynamic behavior of the system can be considered when slowly varying the two essential factors during a long period of time; the current will be evaluated as function of time.

The PV module parameters at different temperature and irradiation conditions are defined by the following way (Chouder et al., 2012):

The ideality factor:

$$V_t = V_{tref}(T/T_{ref}) \quad (40)$$

where T and T_{ref} are the cell and reference temperatures respectively.

The saturation current of the diode:

$$I_0 = I_{0ref}(T/T_{ref})^3 e^{\left(\frac{E_{gap}N_s}{V_{tref}\left(1-\frac{T_{ref}}{T}\right)}\right)} \quad (41)$$

where E_g is the band gap energy of semi conductor (1.12 eV for Si) and N_s is the number of series solar cells composed the PV module.

The photo-current:

$$I_{ph} = (G/G_{ref})(I_{phref} + \alpha_{Isc}(T - T_{ref})) \quad (42)$$

where G and G_{ref} are respectively the solar irradiances at real conditions and at Standard test conditions (STC) (W/m^2); αI_{sc} is the temperature coefficient of short circuit current (A/°C).

The serie resistance:

$$R_s = R_{sref} - \left[\left(\frac{V_t}{I_0}\right)e^{(-V_{0c}/V_t)}\right] \quad (43)$$

where V_{0c} is the voltage which represents the open circuit point; it is expressed by the following relation:

$$V_{0c} = V_{0cref} - \beta(T_{ref} - T) + V_t \ln(G/G_{ref}) \quad (44)$$

The shunt resistance:

$$R_{sh} = R_{shref}(G_{ref}/G) \quad (45)$$

The short circuit current:

$$I_{sc} = I_{scref}(G/G_{ref}) + \alpha I_{sc}(T - T_{ref}) \quad (46)$$

The maximum power point current:

$$I_m = I_{mref}(G/G_{ref}) \quad (47)$$

The maximum power point voltage:

$$V_m = V_{mref} - \beta(T_{ref} - T) \quad (48)$$

where β is the temperature coefficient of the open circuit voltage (V/°C).

The maximum power generated by the photovoltaic system can be obtained as follows:

$$P_m = I_m V_m \quad (49)$$

The effect of the variation of both temperature and solar radiation is highlighted. Fig. 6 presents the current-voltage and the power-voltage characteristics at different irradiances (200 W/m^2, 400 W/m^2, 600 W/m^2, 800 W/m^2 and 1000 W/m^2) and fixed temperature (25 °C). The current-voltage and the power-voltage characteristics at different temperatures (−5 °C, 10 °C, 25 °C, 50 °C and 75 °C) and fixed solar radiation (1000 W/m^2) are shown in Fig. 7.

5. Experimental validation

The experimental test bench is used for the implementation of current-voltage and power-voltage characteristics of the photovoltaic panel TITAN-12-50. The measurement of the voltage and the current is necessary to determine the different parameters of the equivalent electrical circuit of the photovoltaic generator. These quantities are measured by a voltage sensor type LV25-P and a current sensor type LA25-NP.

The solar irradiance is measured from an irradiation sensor based on TLO82 and the temperature is measured from a temperature sensor type LM335 which are carried out in our research unit. The variation of the voltage and the current is made thanks to a variable resistance. To visualize and record this variation, we used a digital storage oscilloscope type scopiX, II (OX 7104). The experimental test bench used in this work is shown in Fig. 8.

6. Results and discussion

6.1. Models validation and analysis

To validate the different models established in this work, experimental tests are all made by varying in each time the solar radiation and the temperature and take the corresponding I-V and P-V characteristics. For this reason, four different tests are carried out and their data are recorded and shown in Figs. 9–12. These four cases cover a large margin that includes different temperature values (from 18 °C to 23.87 °C) and a great variation in solar irradiance (from 366 W/m^2 to 902 W/m^2). A comparative study of the various proposed models with these data is accomplished. The simulation results of each proposed model and the equivalent experimental data are presented in Figs. 9–12.

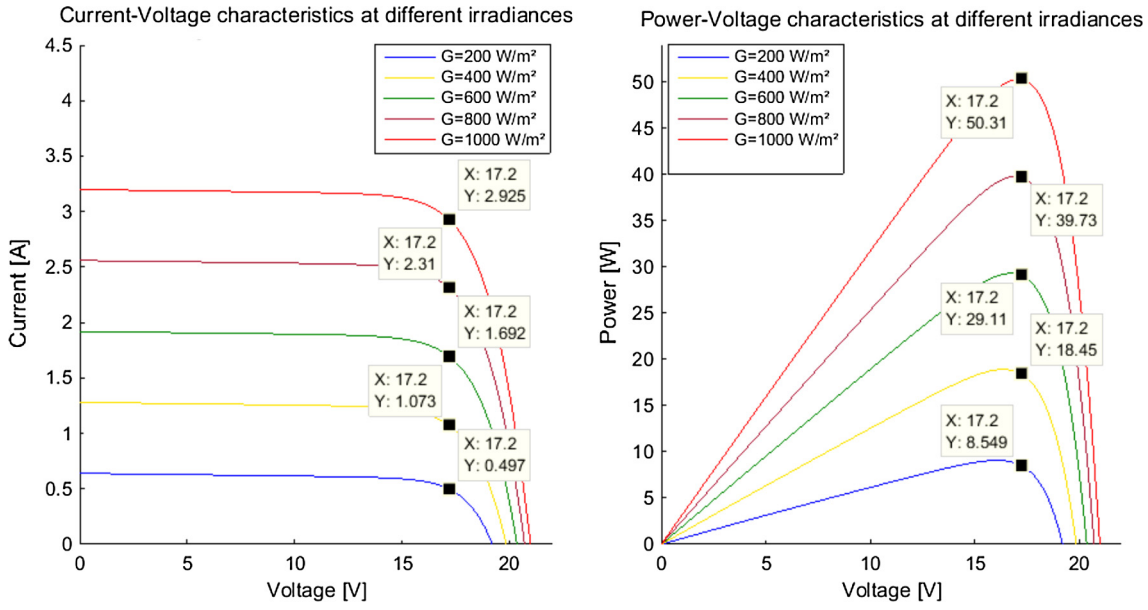

Fig. 6. I-V, P-V characteristics at different irradiances and fixed temperature (25 °C).

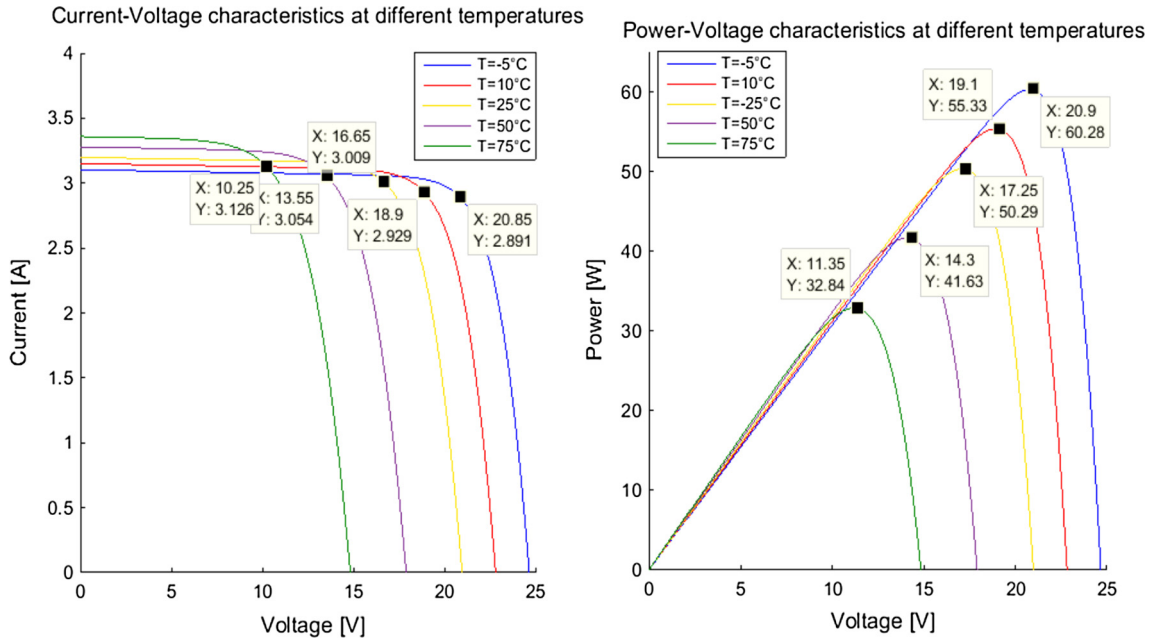

Fig. 7. I-V, P-V characteristics at different Temperatures and fixed radiation (1000 W/m^2).

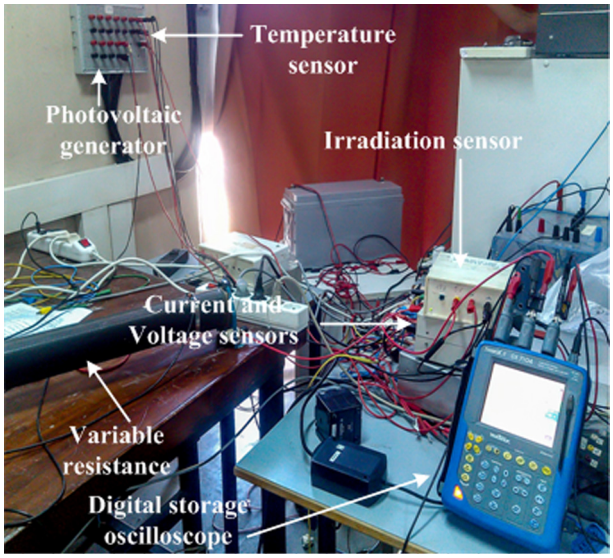

Fig. 8. Experimental test bench.

Fig. 9 shows the experimental data and the different proposed models characteristics at G = 366 W/m^2, T = 18 °C. In this figure, we can conclude that the GA model is more appropriate to describe the real characteristics of the PV panels. The different parameters of the PV panel extracted in this case are summarized in Table 2. The current-voltage and the power-voltage curves of this case are shown in Fig. 8 as follows:

Fig. 10 presents the current-voltage and the power-voltage of the experimental data and the different proposed models at G = 556.7 W/m^2, T = 20.43 °C. In this figures, we can say that the GA model is more appropriate to describe the real characteristics of the PV panels. The GA correctly follows the actual characteristics of our module in all the points describing the current-voltage and power-voltage variations. However, the only difference between the GA model and the other two models exists at the maximum power point. The different parameters of the PV panel acquired in this case are illustrated in Table 2.

Figs. 11 and 12 show the characteristics of the current-voltage and power-voltage at G = 810.2 W/m^2, T = 22.10 °C and G = 902 W/m^2, T = 23.87 °C, respectively. The five different parameters of these two tests and others parameters which are obtained by mathematical manipulations are given in Table 2. In these cases, almost the same result of the previous test (G = 745.2 W/m^2, T = 22.10 °C) was obtained. The only difference is located in the point of the short circuit current. In this point all models are almost confused with the experimental data. But the analytical model does not remain near the point of maximum power as shown in Fig. 12.

The major advantage of this study is to respond seriously to the needs of investors in the field of photovoltaic energy. For this, different models are used in our work and a major improvement in terms of the choice of the parameters constituting the solar cell has been reached. In the various cases of previous tests, the genetic algorithm shows a good performance and accuracy to find in most cases the same real aspect of the static characteristics of the photovoltaic module.

The fitness evolution of the used GA model is shown in Fig. 13. This figure indicates an overall convergence of this algorithm from the iteration 60 and therefore the parameters of our objective function have been delivered. The fitness value of the used function such as the best and mean fitness and their average error are shown in Fig. 13a and b, respectively. The next section discusses precisely and accurately the performance of the various models used in this work.

6.2. Accuracy and performance evaluation of the models

In order to quantify the accuracy and the goodness of the proposed models over current-voltage Characteristics, a root mean square error analysis was applied in general conditions. In this part, two specifics test conditions are taken account, which are (G = 366 W/m^2, T = 18 °C) and (G = 902 W/m^2, T = 23.87 °C). The root mean square error values were obtained using the following equations as follows:

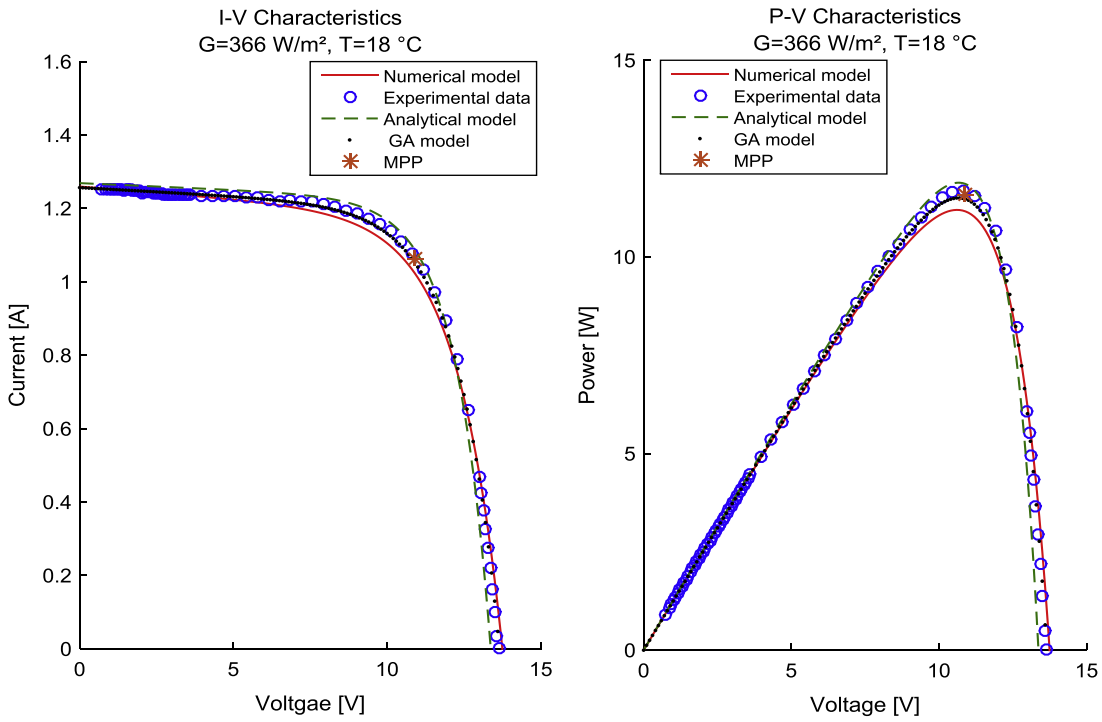

Fig. 9. I-V, P-V characteristics at (G = 366 W/m^2, T = 18 °C).

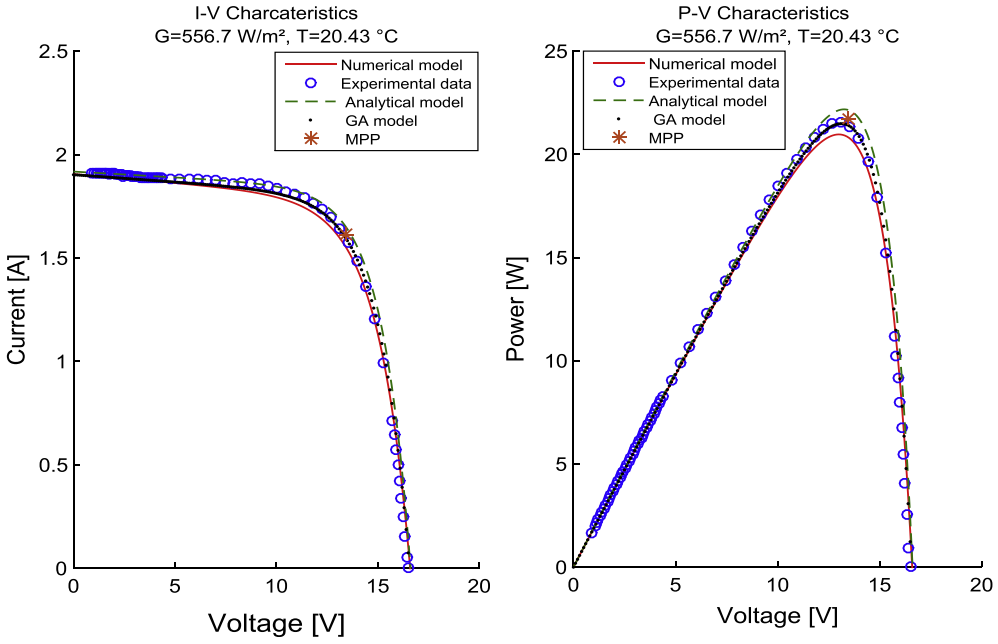

Fig. 10. I-V, P-V characteristics at (G = 556.7 W/m^2, T = 20.43 °C).

$$\mathrm{RMSE}\ (\%) = 100\frac{\sqrt{\frac{1}{M}\sum_{1}^{M}(I_{exp}-I_{mod})^2}}{I_{mod}} \tag{50}$$

where I_{mod} is the current value given by the models and I_{exp} is the experimental current value.

Another major factor can be used to evaluate the performance of the different models, which is the mean relative error of obtained parameters. The mean relative error is expressed by:

$$E_X\ (\%) = 100\frac{X_{mod}-X_{exp}}{X_{exp}} \tag{51}$$

where X_{mod}, X_{exp} are the extracted and the experimental parameters, respectively. M is the number of experimental data and $X = [V_{0c}, I_{sc}, V_m, I_m]$ is the all parameters set to compare.

It's found that the different proposed approaches agree very well with the experimental values with some uncertainty which diverges from one to another model at different levels of irradiance and temperature. Nevertheless, compared with the two other

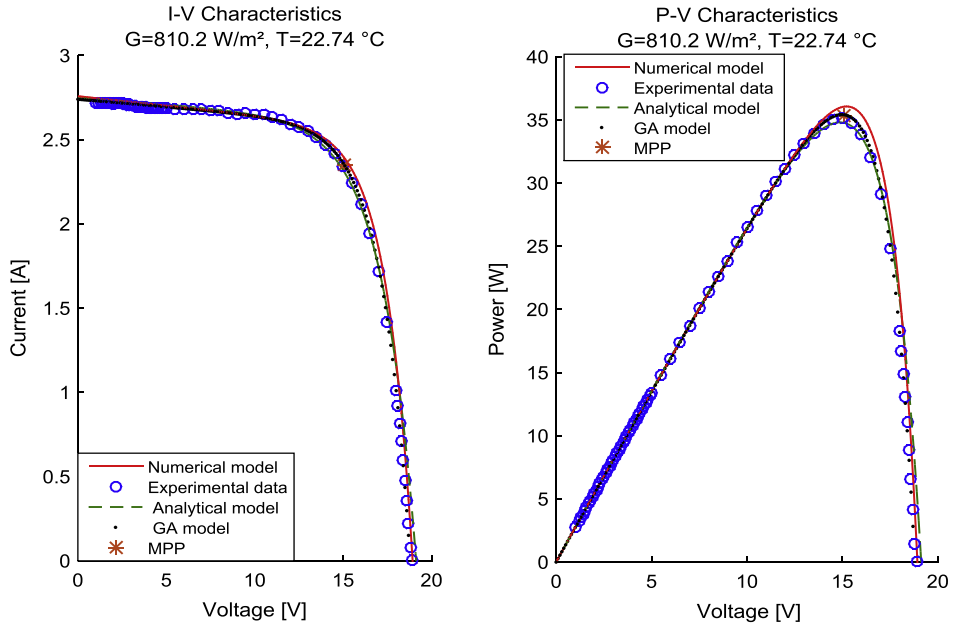

Fig. 11. I-V, P-V characteristics at (G = 810.2 W/m^2, T = 22.74 °C).

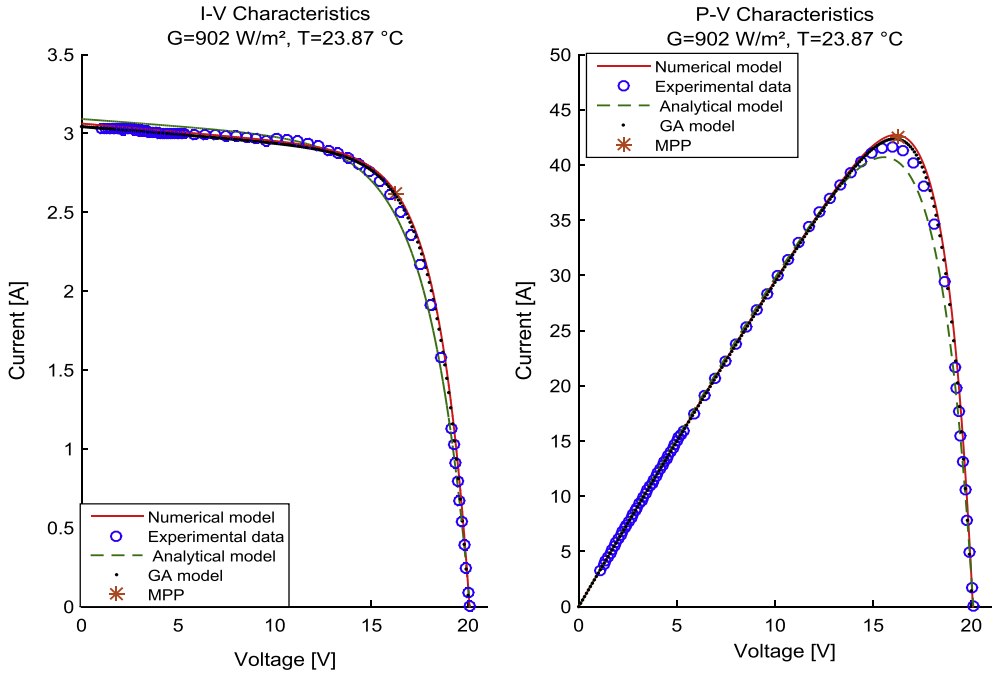

Fig. 12. I-V, P-V characteristics at (G = 902 W/m^2, T = 23.87 °C).

models, the analytical model has a deviation near the neighborhood of maximum power point as mentioned in Figs. 9 and 12. Tables 3 and 4 show the mean relative error E_x for the three characteristic points (V_{0c}, I_{sc}, and MPP) respectively computed with the three proposed models for the used TITAN-12-50 PV module.

In Tables 3 and 4, the E_x of the proposed approaches presents weak errors for our models. Noting that, the GA model shows a good agreement with the experimental data. The E_x of this model is close to 1–2% followed by the numerical model which presents almost the same error that of GA and it varies up to 5%. The difference between these two models is found in the maximum power point and exactly in the V_m point, where the error in this point is less than 1% for the GA and more or less equal to 5% for the numerical model. On the other hand, the analytical model comes in last place and it has an E_x error which can reach 10%.

The root mean square error RMSE of different models is also calculated and has very low errors around 5% for the GA model going to 10% for the analytical model as depicted in Tables 3 and 4.

Figs. 9–12 show the I-V and the P-V curves for the module at different irradiances and temperatures. These figures show a good agreement of I-V and P-V curves with the experimental data of the used solar module.

The recapitulation of this study proves that the proposed GA approach is the most significant and the current-voltage and power-voltage curve of this model exactly corresponds to the experimental values for the different levels of solar irradiance

Table 2
PV panel parameters extracted at (G = 366 W/m^2, T = 18 °C).

Parameters	Analytical model		Numerical model		GA model	
	Reference	General	Reference	General	Reference	General
G = 366 W/m^2, T = 18 °C						
I_{ph} (A)	3.4445	1.2689	3.4193	1.2596	3.4111	1.2566
I_0 (A)	2.5943e−10	1.0630e−05	5.6236e−09	8.9219e−05	1.2334e−09	4.7124e−05
A	0.8264	1.1478	1.0443	1.4506	0.9695	1.3465
R_s (Ω)	0.20	0.4260	0.3123	0.2976	0.4990	0.4661
R_{sh} (Ω)	100	149.1282	54.9979	150.2676	80	218.5792
I_{sc} (A)	3.4377	1.2805	3.4194	1.2668	3.4112	1.2571
V_{0c} (V)	19.2152	13.3714	20.9999	13.7620	20.9912	13.6565
I_m (A)	2.9213	1.0961	2.9370	1.0314	3.0271	1.0614
V_m (V)	17.5133	11.5633	17.9464	11.2500	18.1075	10.9000
Vt (V)	0.0212	0.0295	0.0231	0.0373	0.0269	0.0346
G = 556.7 W/m^2, T = 20.43 °C						
I_{ph} (A)	3.4300	1.9176	3.4086	1.9057	3.4027	1.9024
I_0 (A)	9.1270e−08	1.4856e−05	2.9176e−07	5.1204e−05	8.6583e−08	2.3981e−05
A	1.1587	1.4181	1.2983	1.5887	1.2064	1.4763
R_s (Ω)	0.071	0.0518	0.1667	0.1644	0.30	0.2961
R_{sh} (Ω)	100	179.6299	65.8808	118.3417	80	143.7039
I_{sc} (A)	3.4275	1.9227	3.4092	1.9074	3.4031	1.9018
V_{0c} (V)	20.1393	15.4243	20.9881	16.1849	20.9905	16.3878
I_m (A)	2.9066	1.6181	2.9521	1.6144	2.9950	1.6144
V_m (V)	18.3604	14.4759	17.4010	13.3155	17.6031	13.4526
Vt (V)	0.0298	0.0364	0.0370	0.0408	0.0335	0.0379
G = 810.2 W/m^2, T = 22.74 °C						
I_{ph} (A)	3.3865	2.7503	3.3963	2.7583	3.3738	2.7400
I_0 (A)	1.9059e−05	1.3655e−04	5.9998e−07	9.2357e−06	1.5854e−06	2.2088e−05
A	1.7453	1.9418	1.3584	1.5113	1.4484	1.6114
R_s (Ω)	0.30	0.2998	0.1364	0.1351	0.102	0.101
R_{sh} (Ω)	100	123.4263	72.4197	89.38	90	111.0836
I_{sc} (A)	3.3764	2.7436	3.3960	2.7546	3.3741	2.7384
V_{0c} (V)	20.9798	18.4206	20.9817	18.5314	20.9912	18.5103
I_m (A)	2.9098	2.3575	2.9314	2.3495	2.9192	2.3495
V_m (V)	17.5450	15.3945	17.424	15.0495	17.3953	15.0475
Vt (V)	0.0448	0.0499	0.0349	0.0387	0.0372	0.0414
G = 902 W/m^2, T = 23.87 °C						
I_{ph} (A)	3.4261	3.0936	3.3919	3.0627	3.3706	3.0436
I_0 (A)	9.3408e−05	2.0575e−04	3.5362e−06	1.0561e−05	4.0513e−06	1.2237e−05
A	1.8625	1.9506	1.5331	1.6055	1.5487	1.6220
R_s (Ω)	0.4	0.3999	0.0491	0.0487	0.018	0.0177
R_{sh} (Ω)	100	110.86	85.6775	94.9861	90	99.77
I_{sc} (A)	3.4103	3.0817	3.3921	3.0613	3.3710	3.0433
V_{0c} (V)	20.9455	20.1041	21.0120	20.0839	20.9813	20.0522
I_m (A)	2.8317	2.5542	2.8810	2.6158	2.8723	2.6158
V_m (V)	17.4367	16.4762	17.4102	16.2395	17.4087	16.2135
Vt (V)	0.0478	0.0501	0.0395	0.0412	0.0398	0.0417

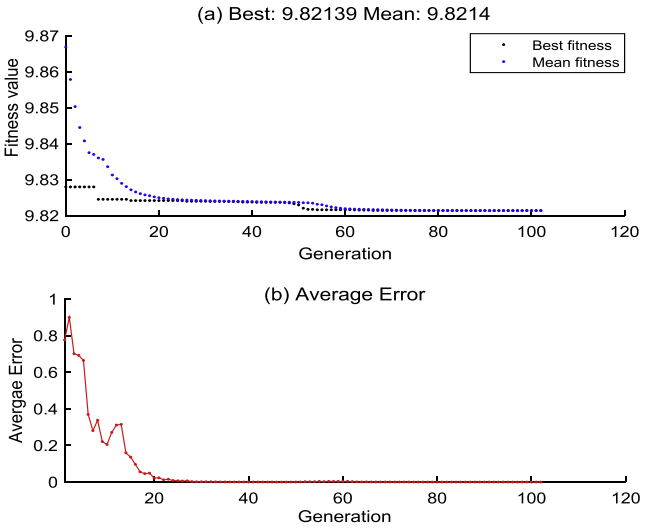

Fig. 13. Fitness function evolution.

Table 3
RMSE and mean relative error at (G = 366 W/m^2, T = 18 °C).

Error	Analytical model	Numerical model	GA model
G = 366 W/m^2, T = 18 °C			
E_{V0c} (%)	−1.5453	1.2509	0.4415
E_{Isc} (%)	0.8744	0.1590	−0.0795
E_{Im} (A)	−0.3728	−1.0997	−1.0811
E_{Vm} (V)	6.7710	3.8781	0.6464
RMSE (%)	9.8712	8.8559	4.8074

Table 4
RMSE and mean relative error at (G = 902 W/m^2, T = 23.87 °C).

Error	Analytical model	Numerical model	GA model
G = 902 W/m^2, T = 23.87 °C			
E_{V0c} (%)	0.1046	0.0458	−0.0175
E_{Isc} (%)	1.3994	0.3244	−0.2655
E_{Im} (%)	−1.3022	1.1245	1.0781
E_{Vm} (%)	1.5764	0.1171	−0.0432
RMSE (%)	9.0529	5.5430	3.0062

and temperature. After comparison, the results obtained indicate the durability, the accuracy and the satisfactory performance of the proposed GA model to significantly reduce the error in the extracted parameters for solar panels.

7. Conclusions

This paper has presented accurately the modeling of an electrical equivalent circuit of a single diode model. The developed models which describe the integral system have been designed to develop a static behavior of photovoltaic generator. An analytical and numerical based Newton-Raphson algorithm models have been mainly used to determine the five parameters of the PV panel. Furthermore, a genetic algorithm model has been applied to improve the performance of the parameters extraction. These previous three models were designed to adapt to the variations in solar radiation and temperature and to ensure a more reasonable I-V and P-V characteristics. Convincing obtained results since the formulated approaches were considered as an optimization problem in determining the five dominating parameters of the single diode model. These different developed models were experimentally validated; their accuracy and performance were discussed. Furthermore, it has been proven that the GA approach has a more satisfactory performance compared with the two other models and its RMSE and E_X for different particular points do not exceed 5% and 1% respectively.

References

Abbassi, R., Chebbi, S., 2012. Energy management strategy for a grid-connected wind-solar hybrid system with battery storage: policy for optimizing conventional energy generation. Int. Rev. Electr. Eng. 7, 3979–3990.

Abbassi, Abdelkader, Ali Dami, Mohamed, Jemli, Mohamed, 2017. A statistical approach for hybrid energy storage system sizing based on capacity distributions in an autonomous PV/Wind power generation system. Renew. Energy 103, 81–93.

Appelbaum, J., Peled, A., 2014. Parameters extraction of solar cells – a comparative examination of three methods. Sol. Energy Mater. Sol. Cells 122, 164–173.

Askarzadeh, Alireza, dos Santos Coelho, Leandro, 2015. Determination of photovoltaic modules parameters at different operating conditions using a novel bird mating optimizer approach. Energy Convers. Manage. 89, 608–614.

Ayodele, T.R., Ogunjuyigbe, A.S.O., Ekoh, E.E., 2016. Evaluation of numerical algorithms used in extracting the parameters of a single-diode photovoltaic model. Sust. Energy Tech. Assess. 13, 51–59.

Batzelis, Efstratios I., Papathanassiou, Stavros A., 2016. A method for the analytical extraction of the single-diode PV model parameters. IEEE Trans. Sust. Energy 7, 504–512.

Bellia, Habbati, Youcef, Ramdani, Fatima, Moulay, 2014. A detailed modeling of photovoltaic module using MATLAB. NRIAG J. Astr. Geophys. 3, 53–61.

Bogning Dongue, Sakaros, Njomo, Donatien, Ebengai, Lessly, 2013. An improved nonlinear five-point model for photovoltaic modules. Int. J. Photoenergy 2013,. http://dx.doi.org/10.1155/2013/680213. 11 p 680213.

Bonkoungou, Dominique, Koalaga, Zacharie, Njomo, Donatien, Zougmore, François, 2015. An improved numerical approach for photovoltaic module parameters acquisition based on single-diode model. Int. J. Cur. Eng. Technol. 5, 3735–3742.

Chikh, Ali, Chandra, Ambrish, 2015. An optimal maximum power point tracking algorithm for PV systems with climatic parameters estimation. IEEE Trans. Sust. Energy 6, 644–652.

Chouder, Aissa, Silvester, Santiago, Sadaoui, Nawel, Rahmani, Lazhar, 2012. Modeling and simulation of a grid connected PV system based on the evaluation of main PV module parameters. Simul. Model Pract. Theory 20, 46–58.

Ciulla, Giuseppina, Brano, Valerio Lo, Dio, Vincenzo Di, Cipriani, Giovanni, 2014. A comparison of different one-diode models for the representation of I-V characteristic of a PV cell. Renew. Sust. Energy Rev. 32, 684–696.

Dongue, S.B., Njomo, D., Tamba, J.G., Ebengai, L., 2012. Modeling of electrical response of illuminated crystalline photovoltaic modules using four- and five-parameter models. Int. J. Emerg. Technol. Adv. Eng. 2, 612–619.

Hejri, Mohammad, Mokhtari, Hossein, Azizian, Mohammad Reza, Ghandhari, Mehrdad, Soder, Lennart, 2014. On the parameter extraction of a five-parameter double-diode model of photovoltaic cells and modules. IEEE J. Photovolt. 4, 915–923.

Humada, Ali M., Hojabri, Mojgan, Mekhilef, Saad, Hamada, Hussein M., 2016. Solar cell parameters extraction based on single and double-diode models: a review. Renew. Sust. Energy Rev. 56, 494–509.

Ishaque, Kashif, Salam, Zainal, 2011. An improved modeling method to determine the model parameters of photovoltaic (PV) modules using differential evolution (DE). Sol. Energy 85, 2349–2359.

Ishaque, Kashif, Salam, Zainal, Taheri, Hamed, 2011a. Simple, fast and accurate two-diode model for photovoltaic modules. Sol Energy Mater. Sol. Cells 95, 586–594.

Ishaque, Kashif, Salam, Zainal, Taheri, Hamed, Shamsudin, Amir, 2011b. A critical evaluation of EA computational methods for Photovoltaic cell parameter extraction based on two diode model. Sol. Energy 85, 1768–1779.

Ishaque, Kashif, Salam, Zainal, Syafaruddin, 2011c. A comprehensive MATLAB Simulink PV system simulator with partial shading capability based on two-diode model. Sol Energy 85, 2217–2227.

Ismail, M.S., Moghavvemi, M., Mahlia, T.M.I., 2013. Characterization of PV panel and global optimization of its model parameters using genetic algorithm. Energy Convers. Manage. 73, 10–25.

Jordehi, A. Rezaee, 2016. Parameter estimation of solar photovoltaic (PV) cells: a review. Renew. Sust. Energy Rev. 61, 354–371.

Lineykin, Simon, Averbukh, Moshe, Kuperman, Alon, 2014. An improved approach to extract the single-diode equivalent circuit parameters of a photovoltaic cell/panel. Renew. Sust. Energy Rev. 30, 282–289.

Lo Brano, Valerio, Ciulla, Giuseppina, 2013. An efficient analytical approach for obtaining a five parameters model of photovoltaic modules using only reference data. Appl. Energy 111, 894–903.

Ma, Tao, Yang, Hongxing, Lin, Lu, 2014. Development of a model to simulate the performance characteristics of crystalline silicon photovoltaic modules/strings/arrays. Sol. Energy 100, 31–41.

Mares, Oana, Paulescu, Marius, Badescu, Viorel, 2015. A simple but accurate procedure for solving the five-parameter model. Energy Convers. Manage. 105, 139–148.

Peng, Wei, Zeng, Yun, Gong, Hao, Leng, Yong-qing, Yan, Yong-hong, Wei, Hu, 2013. Evolutionary algorithm and parameters extraction for dye-sensitised solar cells one-diode equivalent circuit model. IET Mic. Nano Lett. 8, 86–89.

Salaux, Etienne, Teyssedou, Alberto, Sorin, Mikhail, 2011. Explicit model of photovoltaic panels to determine voltages and currents at the maximum power point. Sol Energy 85, 713–722.

Siddiqui, M.U., Abido, M., 2013. Parameter estimation for five- and seven-parameter photovoltaic electrical models using evolutionary algorithms. Appl. Sof. Comput. 13, 4608–4621.

Silva, Emerson A., Bradaschia, Fabricio, Cavalcanti, Marcelo C., Nascimento, Aguinaldo J., 2016. Parameter estimation method to improve the accuracy of photovoltaic electrical model. IEEE J. Photovolt. 6, 278–285.

Singh, Khomdram Jolson, Kho, K.L. Rita, Singh, Sapam Jitu, 2014. Artificial neural network approach for more accurate solar cell electrical circuit model. Int. J. Comput. Sci. Appl. 4.